

1 Revision 1

2

3 Influence of intensive parameters and assemblies on friction
4 evolution during piston-cylinder experiments

5

6

Authors

7 Pierre Condamine*¹, Simon Tournier¹, Bernard Charlier², Etienne Médard³, Antoine
8 Triantafyllou⁵, Célia Dalou¹, Laurent Tissandier¹, Delphine Lequin¹, Camille Cartier¹, Evelyn Füre¹,
9 Pete G. Burnard¹, Sylvie Demouchy⁴, Yves Marrocchi¹

10

11

Affiliations

12 ¹*Université de Lorraine, CNRS, CRPG, F-54000 Nancy, France*

13 ²*Department of Geology, University of Liège, 4000 Sart Tilman, Belgium*

14 ³*Université Clermont Auvergne, CNRS, IRD, OPGC, Laboratoire Magmas et Volcans, F-63000
15 Clermont-Ferrand, France*

16 ⁴*Géosciences Montpellier, CNRS, Université de Montpellier, F-34095 Montpellier, France*

17 ⁵*Geology laboratory of Lyon - Earth, Planets and Environment (LGL-TPE), Université Lyon 1, ENS
18 de Lyon, CNRS, UMR 5276, Villeurbanne, France*

19

20

Correspondence (*)

21 pierre.condamine@univ-lorraine.fr

22

23

Abstract

24 Piston-cylinder assemblies exhibit inhomogeneous pressure distributions and biases compared
25 to the theoretical pressure applied to the hydraulic press because of the thermal and mechanical

26 properties of the assembly components. Whereas these effects can partially be corrected by
27 conventional calibration, systematic quantification of friction values remain very sparse and results
28 vary greatly among previous studies. We performed an experimental study to investigate the behavior
29 of the most common cell assemblies, i.e., talc ($\text{Mg}_3\text{Si}_4\text{O}_{10}(\text{OH})_2$), NaCl, and BaCO_3 , during piston-
30 cylinder experiments to estimate the effects of pressure, temperature, run duration, assembly size, and
31 assembly materials on friction values. Our study demonstrates that friction decreases with time and
32 also partially depends on temperature but does not depend on pressure. We determined that friction
33 decreases from 24 to 17% as temperature increases from 900 to 1300 °C when using talc cells,
34 indicating a friction decrease of ~2% per 100 °C increase for 24-h experiments. In contrast, friction
35 becomes independent of time above 1300 °C. Moreover, at a fixed temperature of 900 °C, friction
36 decreases from 29% in 6-h runs to 21% in 48-h runs, corresponding to a decrease of friction of 0.2%
37 per hour. Similar results obtained with NaCl cell assemblies suggest that friction is constant within
38 error, from 8% in 9-h runs to 5% in 24-h runs. At 900 °C, possible steady-state friction values are only
39 reached after at least 48 h, indicating that friction should be considered a variable for shorter
40 experiments. We establish that assembly materials (and their associated thermomechanical properties)
41 influence the friction correction more than the dimensions of the assembly parts. Finally, we show that
42 the use of polytetrafluoroethylene film instead of conventional Pb foil does not modify friction, but
43 significantly reduces the force required for sample extraction, thus increasing the lifetime of the
44 carbide core, which in turn enhances experimental reproducibility.

45

46

Keywords

47

Experimental petrology | Piston-cylinder | Friction | Assembly | Calibration

48

49

1. Introduction

50

The piston-cylinder apparatus (Boyd and England 1960) is well established in experimental
51 petrology and mineralogy for the synthesis of high-pressure and high-temperature geomaterials.
52 Typical setups can attain pressures of 0.5–4 GPa and temperatures of 600–2000 °C, and special setups

53 extend these ranges down to 0.3 GPa (e.g., Mirwald et al. 1975; Moore et al. 2008) and up to 2500 °C
54 (Cottrell and Walker 2006). Piston-cylinders are thus particularly well suited to investigate material
55 properties at crustal to upper mantle conditions on Earth and even at core conditions on smaller
56 planetary bodies. Furthermore, many thermodynamic models concerning the properties of the mantle
57 and their evolution through geological time rely on experimental databases. It is thus critical to
58 provide accurate experimental data with minimal uncertainties.

59 During high-pressure and high-temperature (*HP-HT*) piston-cylinder experiments, multiple
60 factors can lead to important biases on the pressure applied to the sample. Laboratories worldwide
61 employ various pressurization and heating procedures to reach the *P-T* conditions of interest, such as
62 the commonly used hot piston-in and piston-out techniques, leading to noticeably different applied
63 pressures (Johannes et al. 1971; Shimizu and Kushiro 1984; McDade et al. 2002). It has also been
64 suggested that a fraction of the hydraulic pressure is not transmitted to the sample due to
65 heterogeneous pressure distributions and/or frictional strain between the carbide core and the cell
66 assembly (Tamayama and Eyring 1967; Edmond and Paterson 1971). These pressure losses can be
67 characterized by the friction value *F* (in %), defined as the difference between the applied hydraulic
68 pressure P_{app} and the effective pressure on the sample P_{eff} :

$$69 \quad F = \left(\frac{P_{app}}{P_{eff}} - 1 \right) \times 100 \quad (1)$$

70 The materials used in piston-cylinder cell assemblies vary widely depending on the purpose of
71 the experiments (see Dunn 1993 for a review). For instance, different spacer and sleeve materials can
72 be used around the sample, each possessing unique thermal and mechanical properties (Bell et al.
73 1971; Longhi 2005). Alumina is sometimes substituted for MgO spacers to complete graphite furnaces
74 (Johannes et al. 1971; McDade et al. 2002); however, the different rheological properties of alumina
75 and MgO (elasticity, ductility, hardness) can lead to over- and under-pressured zones around the
76 sample. Furthermore, assemblies made with high-strength materials require greater pressure
77 corrections than those made with low-strength materials (Johannes, 1978). It is therefore important to
78 understand and quantify the role of material properties such as hardness, density, isothermal
79 compressibility, and thermal expansion during *HP-HT* experiments.

80 Several studies have sought to (i) understand and model thermal uncertainties and
81 reproducibility during piston-cylinder experiments (e.g., Watson et al. 2002; Médard et al. 2008) and
82 (ii) estimate the friction correction required depending on cell materials, including the commonly used
83 talc, NaCl, and BaCO₃ pressure media (e.g., Fram and Longhi 1992; Bose and Ganguly 1995; McDade
84 et al. 2002; Longhi 2005). However, the reproducibility of pressure and associated corrections (i.e.,
85 friction) during *HP-HT* experiments and which parameters control their evolution remain unclear. For
86 example, Fram and Longhi (1992) claimed that the friction correction is highly dependent on pressure
87 for BaCO₃ cells, whereas McDade et al. (2002) reported that friction is independent of temperature
88 and pressure at 1000–1600 °C and 1.5–3 GPa. Therefore, the main objective of this study is to
89 experimentally quantify the friction induced by the use of talc, NaCl, and BaCO₃ cells during piston-
90 cylinder experiments. Whereas the use of talc cells is known to produce important pressure losses on
91 the sample compared to the applied hydraulic pressure, friction values are only sparsely reported and
92 vary widely (Johannes et al. 1971; McDade et al. 2002). Our second aim, then, is to understand and
93 quantify the roles of experimental parameters (pressure, temperature, and experimental duration) and
94 assembly materials and size on friction and its evolution during short- and long-duration experiments.

95

96

2. Methods

97

2.1. Experimental strategy

98 Experiments were performed on three different reactions. First, we chose the quartz-coesite
99 transition for its shallow *P-T* slope (Bose and Ganguly 1995, and references therein), which limits
100 biases due to thermal gradients. This simple reaction precludes problems observed in other commonly
101 used transitions, such as synthesis of the starting material in the fayalite + quartz = ferrosilite transition
102 (see Bohlen et al. 1980). In addition, the kinetics of this transition are remarkably fast (Lathe et al.
103 2005), allowing experiments to be performed over both short (2.5 h) and long durations (48 h), in turn
104 allowing us to investigate the evolution of friction over time. We calibrated the quartz-coesite
105 transition over a wide range of typical piston-cylinder temperatures, i.e., at 900 and 1300 °C, to
106 understand the role of temperature on frictional issues in the three cell types (Figure 1). Second, we

107 investigated the albite ($\text{NaAlSi}_3\text{O}_8$) = jadeite ($\text{NaAlSi}_2\text{O}_6$) + quartz (SiO_2) reaction at 800 and 1000 °C
108 using BaCO_3 cells (Holland 1980). Third, we investigated the anorthite ($\text{CaAl}_2\text{Si}_2\text{O}_8$) + gehlenite
109 ($\text{Ca}_2\text{Al}_2\text{SiO}_7$) + corundum (Al_2O_3) = kushiroite ($3\text{CaAl}_2\text{SiO}_6$) reaction (Hays 1966a, b) at a constant
110 pressure of ~1.3 GPa using talc cells to understand the role of pressure and assembly size (1/2" vs.
111 3/4") on friction at 1300 °C.

112 Because low-temperature and short-duration experiments exacerbate friction (Bose and
113 Ganguly 1995), we performed additional experiments on the roles of assembly size and component
114 materials at 900 °C during 6 h. These experiments included replacing the MgO sleeve around the
115 capsule with an alumina sleeve, using a polytetrafluoroethylene (PTFE) film wrapping the cell, and
116 using higher density MgO spacers (2.8 vs. 2.0 g/cm^3) in the graphite furnace (Table 1). A last series of
117 experiments was performed on a new batch of assemblies (thicker talc cell, thinner Pyrex glass) at
118 more conventional piston-cylinder conditions (1300 °C, 24 h) to understand the potential role of
119 assembly part sizes on the generated friction (batch #2; Table 1, Figure 1d).

120

121 **2.2. Starting materials**

122 For the quartz-coesite calibration experiments, we used analytical grade amorphous SiO_2 (99.9
123 wt% purity) and added 6 wt% H_2O to each capsule with a micro syringe to enhance the reaction
124 kinetics (Lathe et al. 2005). To study the kushiroite = anorthite + gehlenite + corundum reaction, we
125 prepared a mixture based on the stoichiometry of the kushiroite, using analytical grade SiO_2 , Al_2O_3 ,
126 and CaCO_3 powders, ground in ethanol for 1 h, and then decarbonated in a furnace at 1200 °C during
127 24 h. The procedure was repeated to ensure complete decarbonation. Oxide powders were stored in an
128 oven at 110 °C prior to capsule assembly. For the albite = jadeite + quartz reaction, the starting
129 material consisted of a mixture of pure powdered crystals, validated by X-ray diffraction
130 measurements on a Bruker D8-Advance diffractometer with $\text{CuK}\alpha$ radiations (ULiege). Proportions
131 were set during mixture preparation, with 70 wt.% quartz, 20 wt.% jadeite and 10 wt.% albite. The
132 powder's mixture was stored in an oven at 120°C prior to capsule assembly.

133

134 **2.3. Experimental techniques**

135 We performed 38 experiments on identical Voggenreiter Mavo LPC 250-300/50 end-loaded
136 12.7-mm (1/2") and 19.0-mm (3/4") piston-cylinders at three different institutes: the Centre de
137 Recherches Pétrographiques et Géochimiques (CRPG, Nancy, France) for talc cell assemblies, the
138 Laboratoire Magmas et Volcans (LMV, Clermont-Ferrand, France) for NaCl cell assemblies, and the
139 University of Liège (ULiège; Belgium) for BaCO₃ cell assemblies. The talc-based piston-cylinder
140 assembly (Ceramic Substrates and Components Ltd.) comprised a talc cell wrapped in an outer PTFE
141 film, a Pyrex cylinder, a graphite furnace, and inner MgO spacers (Figure 1a). The current was
142 conducted to the graphite heater through a stainless-steel plug, which was electrically isolated with a
143 pyrophyllite sleeve. The use of PTFE film instead of conventional Pb foil for the outer sleeve allows
144 covering the base plug, which tends to drastically decrease the force required to extract the assembly at
145 the end of an experiment from ~35 to ~5 kN, which in turn better preserves the carbide core from
146 fracturing. PTFE is also a more environment- and health-friendly alternative compared to Pb and/or
147 Mo-based lubricants. The NaCl cell assembly was similar to the talc cell assembly (Figure 1b). At
148 ULiège, the assembly is composed of a BaCO₃ cell wrapped in Pb foil, a graphite furnace, and MgO
149 spacers (Figure 1c). Additional details on assembly materials and dimensions are provided in
150 Supplementary Materials 1. Calibrated W₇₄Re₂₆-W₉₅Re₅ thermocouples protected by a 4-bore alumina
151 sleeve were used to control temperature to within 1 °C of the setpoint. Temperature gradients
152 throughout the capsule are estimated to be about 20 °C (Sorbadere et al. 2013). The hot spot is located
153 in the center of the capsule, implying a thermal gradient of about 10 °C/mm. To preclude perforation
154 of the capsule, an Al₂O₃/MgO cap 0.6 mm thick was inserted between the capsule and the
155 thermocouple. During experiments, the pressure was first increased to about 0.7 GPa (1/2" assemblies)
156 or 0.3 GPa (3/4" assemblies) at room temperature. In all experiments, the temperature was then
157 increased to 650 °C at 50 °C/min, held for 15 min to reach the target pressure, and then heated to the
158 target temperature.

159 Several series of experiments were conducted to understand the role of assembly parts on
160 friction in talc cells (Table 1). In experiments V32 and V42, we replaced the MgO sleeve with an
161 alumina sleeve, a method used to preserve the experimental charge because alumina sleeves are harder

162 and denser than MgO sleeves. We also investigated the role of the density of MgO spacers by
163 replacing the conventional spacers (2.0 g/cm^3) with higher density spacers (2.8 g/cm^3) in experiments
164 V109 and V117. In experiments V110 and V116, we tested a last batch of assemblies (batch #2) with
165 thicker talc cells (1.35 mm instead of 0.75 mm) and thinner Pyrex glass cylinders (1 mm instead of 1.6
166 mm; see details in Supplementary Materials 1). Finally, in experiments V39 and V107, Pb foil was
167 used instead of the PTFE film.

168 For quartz-coesite transition experiments, $\text{Au}_{80}\text{Pd}_{20}$ capsules (4 mm high) were used to limit
169 water loss (Gaetani and Grove 1998; Kägi et al. 2005). For the kushiroite reaction, Pt capsules (4 mm
170 high) were employed. For the albite = jadeite + quartz reaction, graphite containers (3.75 mm high)
171 were used. At the end of each experiment, the capsule was cut in half longitudinally using a wire saw,
172 mounted in epoxy, and polished to $0.25 \mu\text{m}$ on nylon pads with diamond pastes.

173

174 **2.4. Analytical techniques**

175 Experimental run products of the kushiroite reaction were analyzed with a JEOL JSM-6510
176 scanning electron microscope (SEM) at CRPG using an accelerating voltage of 15 kV, a beam current
177 of 10 nA, and a spot size of $\sim 1 \mu\text{m}$. Back-scattered electron images of experimental run products of
178 the albite = jadeite + quartz reaction were acquired on the QEMSCAN FEI Quanta 650F at RWTH
179 Aachen (Germany).

180 Raman spectroscopy was used to determine the nature of silica polymorphs in all experiments.
181 Raman spectra were acquired using a LabRAM HR spectrometer (Horiba Jobin Yvon) at
182 GeoRessources (Nancy, France). The spectrometer is equipped with a 600 gr/mm grating and an edge
183 filter. The confocal hole aperture is $500 \mu\text{m}$ and the slit aperture is $100 \mu\text{m}$. The excitation beam
184 (wavelength, 514.53 nm; power, 200 mW) was produced by a Stabilite 2017 Ar⁺ laser (Spectra
185 Physics, Newport Corporation) and focused on the sample using a 50 \times objective. The acquisition time
186 (2 s) and the number of accumulated spectra (20) were chosen to optimize the signal-to-noise ratio. All
187 spectra were recorded over Raman shifts of 150–1400 cm^{-1} . Quartz and coesite were identified by
188 their respective peaks at 470 and 520 cm^{-1} .

189

190

3. Experimental textures and products

191

192

193

194

195

196

197

198

Experimental conditions and results of quartz-coesite, kushiroite, and albite reactions are reported in Table 1, and calculated frictions are reported in Table 2. Pictures of typical run products are provided in Supplementary Material 2. In quartz-coesite experiments, coesite was always observed with variable amounts of quartz. Coesite mainly occurs as straight veins in the euhedral quartz matrix, with no preferential orientation. In kushiroite reaction experiments, grain growth was observed in all runs, with anhedral grains ranging from 20 to 50 μm . Kushiroite mainly appears near corundum and anorthite, replacing gehlenite. In runs in which kushiroite was observed (V106 and V113), anorthite, gehlenite and corundum were still present after 24 h.

199

200

201

202

203

204

205

206

207

Non-negligible amounts of the low-pressure phases in the three investigated reactions (i.e., quartz, anorthite + gehlenite + corundum, and albite) persisted after the transition reaction occurred. This result is consistent with Hays (1966a, b), who observed low-pressure phases persisting above the transition to kushiroite, indicating a continuous reaction over a pressure interval of a few kilobars. In contrast to our experiments with a transitional pressure interval of ~ 0.1 GPa, Bose and Ganguly (1995) found only either quartz or coesite in their experiments with a pressure interval of ~ 0.05 GPa. We could not estimate modal abundances from our experimental textures due to significant sample losses during cold decompression.

208

4. Roles of intensive parameters on friction

209

210

211

212

213

214

215

216

In the following sections, experiments from Bose and Ganguly (1995) were chosen as the reference pressure (P_{eff}) for the quartz-coesite system. They indeed showed that after 30 h, the friction is null in their assemblies, based on crossed calibrations using high pressure vessel experiments. In the quartz-coesite system, our experiments at both 900 and 1300 $^{\circ}\text{C}$ allow us to investigate the role of temperature on friction (Figure 2). In 24-h experiments in talc cells, the quartz-coesite transition occurred between applied pressures of 3.68 and 3.77 GPa at 900 $^{\circ}\text{C}$ and between 3.77 and 3.87 GPa at 1300 $^{\circ}\text{C}$. In contrast, Bose and Ganguly (1995) observed the transition at 3.00 and 3.28 GPa at 900 and 1300 $^{\circ}\text{C}$, respectively, in CsCl cells. Taking their values as the effective pressure on the sample,

217 our results indicate friction values (F) for talc cells of 24.1% at 900 °C and 16.5% at 1300 °C (Table
218 1). A linear fit to these values (Figure 2) shows that friction decreases by about 2% when temperature
219 increases by 100 °C in 24-h experiments. In NaCl cells, the quartz-coesite transition occurred between
220 3.11 and 3.21 GPa at 900 °C ($F = 5.4 \pm 3.0\%$) and between 3.41 and 3.46 GPa at 1300 °C ($F = 4.8 \pm$
221 3.0%), indicating no friction evolution within error. In BaCO₃ cells, the albite = jadeite + quartz
222 reaction occurred between 2.35 and 2.4 GPa at 800 °C and between 2.8 and 2.9 GPa at 1000 °C.
223 Compared to 2.16 and 2.69 GPa at 800 and 1000 °C obtained in Holland (1980), $F = 10.2 \pm 4.3$ and
224 $6.1 \pm 3.4\%$, respectively, indicating no friction evolution in this range of temperature.

225 Our experiments on the kushiroite = anorthite + gehlenite + corundum reaction were
226 conducted at 1300 °C to understand the role of pressure on the friction value in talc cells. In 1/2"
227 assemblies, this transition occurred between applied pressures of 1.45 and 1.54 GPa in 24-h
228 experiments. According to the equation of Hays (1966a), the reference pressure for this transition is
229 1.3 GPa, resulting in a friction value of $15.1 \pm 4.3\%$.

230 This value is identical, within errors, to the friction value obtained from the quartz-coesite
231 transition at the same temperature ($16.6 \pm 3.2\%$), implying that the friction value is independent of
232 confining pressure at identical temperatures and experimental durations. This result is partially
233 consistent with McDade et al. (2002), who argued that the friction correction is independent of
234 pressure and temperature at 1000–1600 °C and 1.5–3.2 GPa in BaCO₃ cells. However, our results
235 show that friction is temperature dependent in talc cells, decreasing by 2% over a temperature increase
236 of 100 °C between 900 and 1300 °C. This difference can be explained by the slower stress
237 accommodation of talc compared to NaCl and BaCO₃ cells due to its higher strength. It is also possible
238 that friction becomes more strongly temperature dependent at low temperature (<1000 °C). We
239 speculate that stress accommodation is fast enough above 1000 °C to be undetectable under these
240 experimental conditions.

241

242

5. Friction evolution

243 We performed experiments on the quartz-coesite reaction at 900 °C and over various run
244 durations between 2.7 and 48 h to investigate the evolution of friction during a single run (Figure 3).

245 In talc cells, the transition occurred at progressively lower applied pressures with increasing run
246 duration (Table 1); friction thus evolved from $33.8 \pm 3.4\%$ after 2.7 h to $30.7 \pm 3.3\%$ after 4.5 h, 27.3
247 $\pm 3.3\%$ after 6 h, $24.1 \pm 3.2\%$ after 24 h, and to $20.9 \pm 3.2\%$ after 48 h (Figure 3). Whereas a linear fit
248 to the data for longer durations (≥ 6 h) indicates that friction decreases by $\sim 2\%$ every 10 h, a power-law
249 fit better describes the full dataset. This may explain the ubiquitous presence of quartz in all
250 experiments conducted in talc cells via the early crystallization of quartz from the amorphous SiO_2
251 starting material at low effective pressures and its subsequent metastability. In contrast, in talc cell
252 assemblies at 1300°C , friction did not evolve between 6- and 24-h duration experiments, indicating
253 that a frictional steady state was achieved within less than 6 h.

254 In NaCl cells at 900°C , the apparent pressure of the quartz-coesite transition decreased from
255 between 3.21 and 3.30 GPa after 9 h ($F = 8.4 \pm 3.1\%$) to between 3.11 and 3.21 GPa after 24 h ($F =$
256 $5.4 \pm 3.0\%$), indicating no friction evolution within error, contrary to what is reported in talc cells over
257 longer duration experiments. The friction decrease in talc cell is however consistent with the data of
258 Bose and Ganguly (1995) in CsCl cell assemblies (both $1/2''$ and $3/4''$), which show that friction
259 decreased from 6.6% after 2 h to negligible after 35 h, or by $\sim 2\%$ every 10 h (Figure 3).

260

261 **6. Thermomechanical properties of assembly components**

262 **Alumina sleeve**

263 Experiments V32 and V42 (Table 1) were performed at 900°C and applied pressures of 3.87
264 and 3.97 GPa, respectively, with an alumina sleeve around the capsule instead of a conventional MgO
265 sleeve. In both experiments, only quartz was observed, and the pressure limitation of the carbide core
266 precludes experiments at pressures above ~ 4 GPa. Thus, the minimum friction observed using alumina
267 sleeves is $>32.3\%$ (Figure 4). However, the main advantage of alumina sleeves is that the sample
268 capsule conserves its cylindrical shape, preventing excessive deformation during quenching and cold
269 depressurization, a net advantage when working with single crystals. McDade et al. (2002) obtained a
270 friction value of 3.6% in NaCl cells by using an alumina sleeve and Alsimag (Al_2O_3) plugs to fill the
271 tapered graphite furnace. Given the high density and hardness of Alsimag, these plugs are better

272 pressure transmitters than the crushable MgO used in our assembly setup. The combination of an
273 alumina sleeve with MgO spacers thus greatly decreases pressure transmission and should only be
274 used to limit fracturing of the experimental product in cases requiring particular care for the capsule.

275

276 **Density of MgO spacers**

277 Experiments V109 and V117 made with talc-Pyrex assemblages were conducted 900 °C and
278 applied pressures of 3.68 and 3.77 GPa, respectively, with higher density MgO spacers (2.8 vs. the
279 usual 2.0 g/cm³). Both coesite and quartz were observed in V117, positioning the apparent quartz-
280 coesite transition at 3.72 GPa. The friction obtained using these MgO spacers ($24.1 \pm 3.2\%$; Figure 4)
281 is identical within error to that obtained using the standard assembly under the same conditions ($27.3 \pm$
282 3.3%). This result demonstrates that the densities of assembly components does not significantly affect
283 the effective sample pressure. This however further highlights that the Alsimag spacers used by
284 McDade et al. (2002) are a good pressure medium, as they achieved a friction value of only 3.6%.

285

286 **Assembly size (1/2" vs. 3/4")**

287 Kushiroite reaction experiments were performed in both 1/2" and 3/4" assemblies at 1300 °C
288 for 24 h (Table 1). The calculated friction values are identical within errors, i.e., $15.1 \pm 4.3\%$ and 15.9
289 $\pm 4.4\%$ for the 1/2" and 3/4" assemblies, respectively (Figure 3), suggesting that the size of assembly
290 parts has a negligible effect on friction compared to assembly materials (and their associated
291 thermomechanical properties).

292 Experiments V110 and V116 were performed using assemblies with thicker talc cells and
293 thinner Pyrex sleeves ('batch #2', see Supplementary Materials 1 for size details). The friction
294 determined for this assembly ($16.6 \pm 3.2\%$) is identical to that for the standard assembly ($16.6 \pm 3.2\%$)
295 at 1300 °C for 24 h (Figure 4), further demonstrating that assembly materials have a stronger influence
296 on friction than their sizes.

297

298 **Pb foil vs PTFE foil**

299 Experiments V107 and V39 were performed at 900 °C and applied pressures of 3.77 and 3.87
300 GPa, respectively, using talc cells and standard Pb foil instead of the PTFE film used elsewhere in this
301 study (excluding ULiège experiments, Table 1). Coesite was only observed in experiment V39,
302 implying that friction ($27.3 \pm 3.3\%$) was identical within errors to that using a PTFE-wrapped
303 assembly ($27.3 \pm 3.3\%$; Figure 4). As previously mentioned, the key advantage of using PTFE film
304 instead of Pb foil is the preservation of the carbide core of the pressure plates. The steel base plug,
305 surrounded by pyrophyllite, is frequently stuck in the carbide core when removing the assembly,
306 especially after experiments run at pressures above 2.0 GPa. The use of Pb foil precludes covering the
307 base plug to avoid melting the Pb at the contact point with the thermocouple plate, which can
308 electrically short-circuit the experiment. Therefore, the use of PTFE film is recommended to limit the
309 development of fractures within the carbide core, which will both extend the life of the carbide core
310 and enhance pressure reproducibility over that lifetime.

311

312 **7. Implications for pressure reproducibility during piston-cylinder experiments**

313 In this section, we provide general recommendations to improve pressure and temperature
314 reproducibility during piston-cylinder experiments. These recommendations can be adapted,
315 depending on the capsule material and the scientific purpose, e.g., for oxygen-fugacity buffering or
316 volatile-bearing experiments. These recommendations are depicted in *P-T-t* space in the form of
317 preferential practices in Figure 5.

318 At temperatures above 1600 °C, the NaCl cell is no longer usable because of the melting point
319 of NaCl. Consequently, only talc or BaCO₃ cells should be used for very-high temperature
320 experiments. Talc cells require a very-high frictional correction factor, regardless of *P-T-t* conditions
321 (Table 2) and should thus be avoided in very high pressure experiments (>3 GPa) because the carbide
322 core could suffer from excessive applied pressure. To generate pressures above 3 GPa, we thus
323 recommend using NaCl cells below 1600 °C because they exhibit the lowest friction corrections
324 (Figures 2 and 3) or BaCO₃ cells at higher temperatures. For experimental durations of a few to ~48 h

325 and pressures below 3 GPa, talc cells are as competent as NaCl and BaCO₃ cells because they all show
326 similar frictional evolution with time. However, for short experiments (≤ 6 h), we recommend using
327 NaCl or BaCO₃ cells as the decrease in friction value with time is comparable and because the friction
328 in talc cells is much greater (following a power law) in shorter duration experiments (Figure 3). As
329 described in section 5, this could lead to unexpectedly low effective pressures, promoting the
330 crystallization and metastability of low-pressure phases. For experiments longer than 48 h (and below
331 1600 °C), we recommend using NaCl cells: whereas friction becomes negligible in CsCl cells after
332 ~30 h (Bose and Ganguly 1995), the behavior of talc cells in experiments longer than 48 h remains
333 unclear. Therefore, for temperatures above 1600 °C and durations longer than 48 h, we recommend
334 using BaCO₃ cells because of their lower frictional correction compared to talc cells.

335

336

8. Conclusions

337 We determined the effects of pressure, temperature, time and assembly parts (materials and
338 size) on the frictional correction factors to be applied to piston-cylinder experiments using talc cell
339 assemblies. Whereas pressure calibrations in most laboratories assume a single value for friction
340 correction for a given assembly, our study demonstrate that friction is time- and temperature-
341 dependent, and particularly elevated friction can be produced for short experiments at low
342 temperature, especially for talc-cell assemblies. Whereas the size of assembly parts has a negligible
343 effect on friction, different sleeve and spacer materials (here, MgO vs. alumina) can significantly
344 change the friction factors. Friction decreases by about 2% per 100 °C increase between 900 and 1300
345 °C at a given duration. Experimental duration also has a strong effect on the friction value at low
346 temperatures, with friction decreasing by about 0.2% per hour at 900 °C; this effect is not observed at
347 1300 °C. In contrast to CsCl cells, in which friction becomes negligible after around 30–35 h, the
348 friction in talc cells, although decreasing with increasing run duration, is never negligible, especially at
349 low temperatures. Therefore, special care must be taken for low-temperature experiments (roughly
350 <1000 °C) using talc cells, especially at short durations, because the slow stress accommodation of the
351 assembly results in slow frictional evolution during the first several hours. Other key parameters not
352 studied here may also critically affect friction and its evolution. In particular, the quality of the carbide

353 core and the development of fractures are expected to influence the friction generated on the assembly.
354 A more systematic calibration procedure including the status of the core is thus necessary to provide a
355 complete model of friction and its evolution during an experiment. This is fundamental for phase
356 relationship experiments or the quest for low-degree melts from mantle lithologies, for which accurate
357 and reproducible *P-T* conditions are essential. Furthermore, a dynamic model for friction correction
358 should be developed to ensure pressure reproducibility among *HP-HT* petrological studies.

359

360

Acknowledgments

361 The authors thank Fred Davis and an anonymous reviewer for their constructive reviews, as
362 well as Kate Kiseeva for her editorial handling. We thank M.-C. Caumon for technical assistance with
363 Raman analyses and P. Baillot for his technical expertise in the laboratory. We also thank K. Koga and
364 F. Faure for fruitful discussions. P.C. thanks C. McCammon for fundamental advice when building the
365 piston-cylinder laboratory at CRPG. This study was mainly financed by l'Agence Nationale de la
366 Recherche through grant ANR INDIGO (ANR-14-CE33-0011). C. Dalou and E. Füre were supported
367 by the European Research Council (ERC) under the European Union's Horizon 2020 research and
368 innovation program (grant agreement no. 715028). B. Charlier is a Research Associate of the Belgian
369 Fund for Scientific Research-FNRS. A. Triantafyllou was supported by the FRS-FNRS for the
370 PROBARC project (Grant CR n°1. B. 414.20F). This is CRPG contribution no. 2747.

371

References

- 372 Bell, P., Mao, H., and England, J. (1971) A discussion of pressure distribution in modern solid-
373 pressure-media apparatus. Carnegie Institution of Washington, Yearbook, 70, 277–281.
- 374 Bohlen, S.R., Essene, E.J., and Boettcher, A.L. (1980) Reinvestigation and application of olivine-
375 quartz-orthopyroxene barometry. Earth and Planetary Science Letters, 47, 1–10.
- 376 Bose, K., and Ganguly, J. (1995) Quartz-coesite transition revisited; reversed experimental
377 determination at 500-1200 degrees C and retrieved thermochemical properties. American
378 Mineralogist, 80, 231–238.
- 379 Boyd, F.R., and England, J.L. (1960) Apparatus for Phase-Equilibrium Measurements at Pressures up
380 to 50 Kilobars and Temperatures up to 1750°C. Journal of Geophysical Research, 65, 741–748.
- 381 Cottrell, E., and Walker, D. (2006) Constraints on core formation from Pt partitioning in mafic silicate
382 liquids at high temperatures. Geochimica et Cosmochimica Acta, 70, 1565–1580.
- 383 Dunn, T. (1993) The Piston-Cylinder Apparatus. In R.W. Luth, Ed., Experiments at High Pressure and
384 Applications to the Earth's Mantle Vol. 21, pp. 39–94.
- 385 Edmond, J.M., and Paterson, M.S. (1971). Strength of solid pressure media and implications for high
386 pressure apparatus. Contributions to Mineralogy and Petrology 30, 141–160.
- 387 Fram, M.S., and Longhi, J. (1992) Phase equilibria of dikes associated with Proterozoic anorthosite
388 complexes. American Mineralogist, 77, 605–616.
- 389 Gaetani, G.A., and Grove, T.L. (1998) The influence of water on melting of mantle peridotite.
390 Contributions to Mineralogy and Petrology, 131, 323–346.
- 391 Hays, J.F. (1966a). Lime-Alumina-Silica. Year book - Carnegie Institution of Washington 65, 234–
392 239.
- 393 Hays, J.F. (1966b) Stability and properties of the synthetic pyroxene $\text{CaAl}_2\text{SiO}_6$. American
394 Mineralogist, 51, 1524–1529.
- 395 Holland, T.J.B. (1980) The reaction albite = jadeite+quartz determined experimentally in the range
396 600–1200 ° C. American Mineralogist, 65, 129–134.
- 397 Johannes, U. (1978) Pressure comparing experiments with NaCl, AgCl, talc, and pyrophyllite
398 assemblies in a piston cylinder apparatus. Neues Jahrbuch für Mineralogie Monatshefte, 84–92.

- 399 Johannes, W., Bell, P.M., Mao, H.K., Boettche, A.I., Chipman, D.W., Hays, J.F., Newton, R.C., and
400 Seifert, F. (1971) Interlaboratory comparison of piston-cylinder pressure calibration using albite
401 breakdown reaction. *Contributions to Mineralogy and Petrology*, 32, 24-.
- 402 Kägi, R., Müntener, O., Ulmer, P., and Ottolini, L. (2005) Piston-cylinder experiments on H₂O
403 undersaturated Fe-bearing systems: An experimental setup approaching fO₂ conditions of natural
404 calc-alkaline magmas. *American Mineralogist*, 90, 708–717.
- 405 Lathe, C., Koch-Müller, M., Wirth, R., Van Westrenen, W., Mueller, H.-J., Schilling, F., and
406 Lauterjung, J. (2005) The influence of OH in coesite on the kinetics of the coesite-quartz phase
407 transition. *American Mineralogist*, 90, 36–43.
- 408 Longhi, J. (2005) Temporal stability and pressure calibration of barium carbonate and talc/pyrex
409 pressure media in a piston-cylinder apparatus. *American Mineralogist*, 90, 206–218.
- 410 McDade, P., Wood, B.J., Van Westrenen, W., Brooker, R., Gudmundsson, G., Soulard, H., Najorka,
411 J., and Blundy, J. (2002) Pressure corrections for a selection of piston-cylinder cell assemblies.
412 *Mineralogical Magazine*, 66, 1021–1028.
- 413 Médard, E., McCammon, C.A., Barr, J.A., and Grove, T.L. (2008) Oxygen fugacity, temperature
414 reproducibility, and H₂O contents of nominally anhydrous piston-cylinder experiments using
415 graphite capsules. *American Mineralogist*, 93, 1838–1844.
- 416 Mirwald, P.W., Getting, I.C., and Kennedy, G.C. (1975) Low-friction cell for piston-cylinder high-
417 pressure apparatus. *Journal of Geophysical Research (1896-1977)*, 80, 1519–1525.
- 418 Moore, G., Roggensack, K., and Klonowski, S. (2008) A low-pressure–high-temperature technique for
419 the piston-cylinder. *American Mineralogist*, 93, 48–52.
- 420 Shimizu, N., and Kushiro, I. (1984) Diffusivity of oxygen in jadeite and diopside melts at high
421 pressures. *Geochimica et Cosmochimica Acta*, 48, 1295–1303.
- 422 Sorbadere, F., Médard, E., Laporte, D., and Schiano, P. (2013) Experimental melting of hydrous
423 peridotite-pyroxenite mixed sources: Constraints on the genesis of silica-undersaturated magmas
424 beneath volcanic arcs. *Earth and Planetary Science Letters*, 384, 42–56.
- 425 Tamayama, M., and Eyring, H. (1967). Study of Pressure Calibration and Pressure Distribution in a
426 Piston-Cylinder High Pressure Press. *Review of Scientific Instruments* 38, 1009–1018.

427 Watson, E.B., Wark, D.A., Price, J.D., and Van Orman, J.A. (2002) Mapping the thermal structure of
428 solid-media pressure assemblies. *Contributions to Mineralogy and Petrology*, 142, 640–652.

429

Figure captions

430

431

432

433

434

435

436

437

438

439

440

441

442

443

444

445

446

447

448

449

450

451

452

453

454

455

456

Figure 1. Schematic diagrams of the four different piston-cylinder cell assemblies used in this study. a) talc cell assembly used at CRPG (Nancy), b) NaCl cell assembly used at LMV (Clermont-Ferrand), c) BaCO₃ assembly used at ULG (Liège), d) batch #2 of the talc cell assembly used at CRPG, using a thicker cell and thinner Pyrex sleeve compared to *a*. The talc cell is 0.75 mm thick in *a* against 1.35 mm in *d*. Contrary to other assemblies, no Pyrex glass is present in the BaCO₃ cell assembly and a Pb film is used instead of PTFE to wrap the cell. See Supplementary Materials 1 for additional details.

Figure 2. Friction evolution as a function of temperature for 24 h experiments in 1/2" cell assemblies. The durations of experiments from McDade et al. (2002) were 22 h. Linear fits describe the change in friction as a function of temperature (°C): $F = -0.019T + 40.991$ for talc cells; $F = -0.006T + 10.370$ for NaCl cells; $F = -0.020T + 26.463$ for BaCO₃ cells.

Figure 3. Evolution of the friction value as a function of experimental duration. B&G1995 data correspond to the study of Bose and Ganguly (1995), performed at 900 °C with CsCl cells. At 900 °C, the friction value decreases of about 2 % every 10 h for experimental durations > 6 h. At 1300 °C, no friction decrease is observed between 6 and 24 h. Lower pressure (kushiroite experiments) and sizing of assemblies (1/2" and 3/4") do not seem to have a critical influence on the friction value and its evolution. The slope of the friction decrease observed in NaCl cell assemblies is comparable to the slope observed in Bose and Ganguly (1995).

Figure 4. Variations in friction with changes in assembly size and components, relative to experiments performed using the assembly shown in Figure 1a (talc cell, MgO sleeve, PTFE film, 2.0 g/cm³ MgO spacers) at 900 °C for 6 h and 1300 °C for 24 h (1/2" assembly). ‘Alumina sleeve’ indicates that the regular MgO sleeve around the capsule was replaced by an alumina sleeve. ‘Pb foil’ indicates that the cell was wrapped in standard Pb foil instead of the PTFE film used throughout this study. ‘MgO spacers’ indicates that higher density MgO spacers (2.8 g/cm³) were used within the

457 graphite furnace (including the sleeve around the capsule). ‘Assembly batch #2’ indicates the
458 assembly shown in Figure 1d, using a thicker talc cell and thinner Pyrex sleeve than those in the
459 regular assembly (Figure 1a). See Supplementary Materials 1 for details. Note that the friction
460 reported for ‘Alumina sleeve’ is a minimum value because coesite was not observed in this series of
461 experiments due to the pressure limitations of the press and carbide core.

462

463 **Figure 5.** Recommended cell types for piston-cylinder experiments as a function of pressure,
464 temperature, and experimental duration. Note that the duration axis is not linear. These general
465 recommendations limit the uncertainty on pressure and its evolution during *HP-HT* experiments,
466 except for avoiding NaCl cells in experiments at very high temperature (>1600 °C) because the NaCl
467 cell no longer acts as an electrical insulator. See discussion in section 7 for further details. Cell types
468 are recommended as ‘best > intermediate > worst’ according to the color scale at bottom right.

Table 1

Experimental conditions and results

Assembly	T (°C)	Duration (h)	Run	P _{app} (GPa)	
Talc cell experiments (CRPG laboratory)					
PTFE - Talc - Pyrex - C - MgO	900	2.7	V130	3.97	
			V16	4.06	
		4	V10	3.87	
		5	V19	3.97	
		6	V108	3.77	
			V55	3.87	
		15	V41	3.77	
			V38	3.87	
		24	V30	3.68	
			V24	3.77	
		48	V33	3.58	
			V56	3.68	
			6	V37	3.77
				V18	3.87
		1300	24	V22	3.77
				V57	3.87
			24	V114	1.45
		V113	1.54		
PTFE - Talc - Pyrex - C - Al ₂ O ₃	900	6	V32	3.87	
			V42	3.97	
Pb - Talc - Pyrex - C - MgO	900	6	V107	3.77	
			V39	3.87	
PTFE - Talc - Pyrex - C - MgO (2800 kg/m ³)	900	6	V109	3.68	
			V117	3.77	
PTFE - Talc - Pyrex - C - MgO (batch #2)	1300	24	V110	3.77	
			V116	3.87	
PTFE - Talc - Pyrex - C - MgO (3/4")	1300	24	V112	1.46	
			V106	1.55	
NaCl cell experiments (LMV laboratory)					
PTFE - NaCl - Pyrex - C - MgO	900	9	PC/2014/11	3.21	
			PC/2014/14	3.30	
		24	Cal-LMV-03	3.11	
			Cal-LMV-01	3.21	
		1300	24	Cal-LMV-02	3.41
				Cal-LMV-04	3.46
BaCO₃ cell experiments (ULG laboratory)					
Pb - BaCO ₃ - C - MgO	800	24	A070	2.35	
			A058	2.40	
	1000	24	A073	2.80	
			A060	2.90	

Product

qz
qz + co
qz
qz + co
qz
qz + co
qz
qz + co
qz
qz + co
qz
qz + co

qz
qz + co
qz
qz + co
an + gh + crn
kush + an + gh + crn

qz
qz
qz
qz + co

qz
qz + co

qz
co

an + gh + crn
kush + an + gh + crn

qz
qz + co
qz
qz + co

qz
qz + co

ab
jd + qz

ab
jd + qz

Table 2

Friction values

Size (")	T (°C)	Duration (h)	P_{app}	ΔP_{app}	P_{eff}	ΔP_{eff}	F (%)	ΔF
Talc cell (CRPG laboratory)								
Friction as a function of temperature								
	900		3.72	0.10	3.00	0.05	24.1	3.2
	1000 ^a		3.75	0.10	3.07	0.06	22.0	3.2
1/2	1100 ^a	24	3.77	0.10	3.14	0.06	20.1	3.2
	1200 ^a		3.79	0.10	3.21	0.06	18.3	3.2
	1300		3.82	0.10	3.28	0.07	16.6	3.2
Friction as a function of duration								
		2.7	4.01	0.10	3.00	0.05	33.8	3.4
		4.5	3.92	0.10	3.00	0.05	30.7	3.3
	900	6	3.82	0.10	3.00	0.05	27.3	3.3
1/2		15	3.82	0.10	3.00	0.05	27.3	3.3
		24	3.72	0.10	3.00	0.05	24.1	3.2
		48	3.63	0.10	3.00	0.05	20.9	3.2
	1300	6	3.82	0.10	3.28	0.07	16.6	3.2
		24	3.82	0.10	3.28	0.07	16.6	3.2
Friction as a function of pressure and assembly size								
1/2	1300	24	1.50	0.10	1.30	0.03	15.1	4.3
3/4			1.51	0.06	1.30	0.03	15.9	4.4
Friction as a function of assembly parts								
			3.82	0.10	3.00	0.05	27.3	3.3
	900	6	> 3.97		3.00	0.05	> 32.2	
1/2			3.82	0.10	3.00	0.05	27.3	3.3
			3.72	0.10	3.00	0.05	24.1	3.2
	1300	24	3.82	0.10	3.28	0.07	16.6	3.2
			3.82	0.10	3.28	0.07	16.6	3.2
NaCl cell (LMV laboratory)								
1/2	900	9	3.25	0.10	3.00	0.05	8.4	3.1
1/2		24	3.16	0.10	3.00	0.05	5.4	3.0
1/2	1300	24	3.38	0.10	3.28	0.07	4.8	3.0
BaCO₃ cell (ULG laboratory)								
1/2	800	24	2.38	0.10	2.16	0.05	10.2	4.3
1/2	1000		2.85	0.10	2.69	0.05	6.1	3.4

P_{app} and P_{eff} represent the pressure (GPa) applied by the press and the pressure of the sample, respectively. ΔP_{app} , ΔP_{eff} and ΔF are 2σ standard deviations of applied pressure, effective pressure and friction, respectively.

^aValues from the linear fit in Figure 2.

Comment

Standard calibration (900 °C, 6 h)

Alumina sleeve

Pb foil

MgO spacers density

Standard calibration (1300, 24 h)

Assembly batch #2

in the sample, respectively. F

lied pressure, sample pressure and

Fig. 1

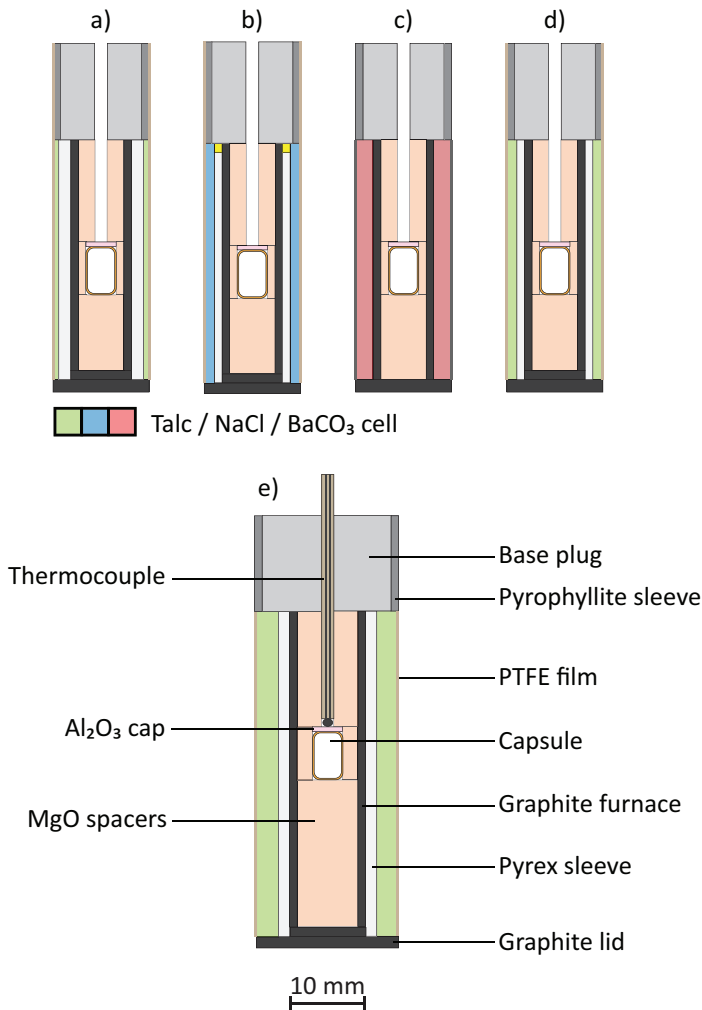


Fig. 2

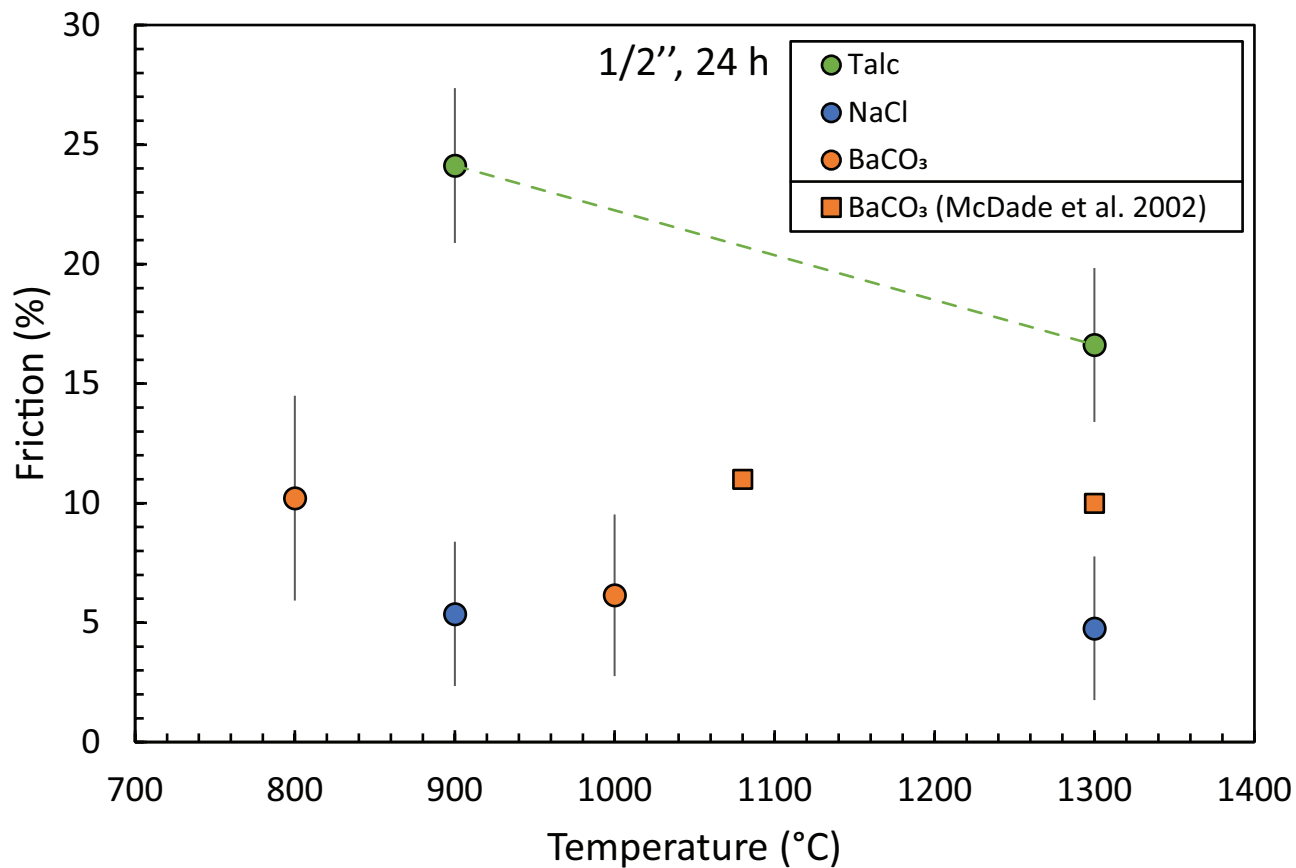


Fig. 3

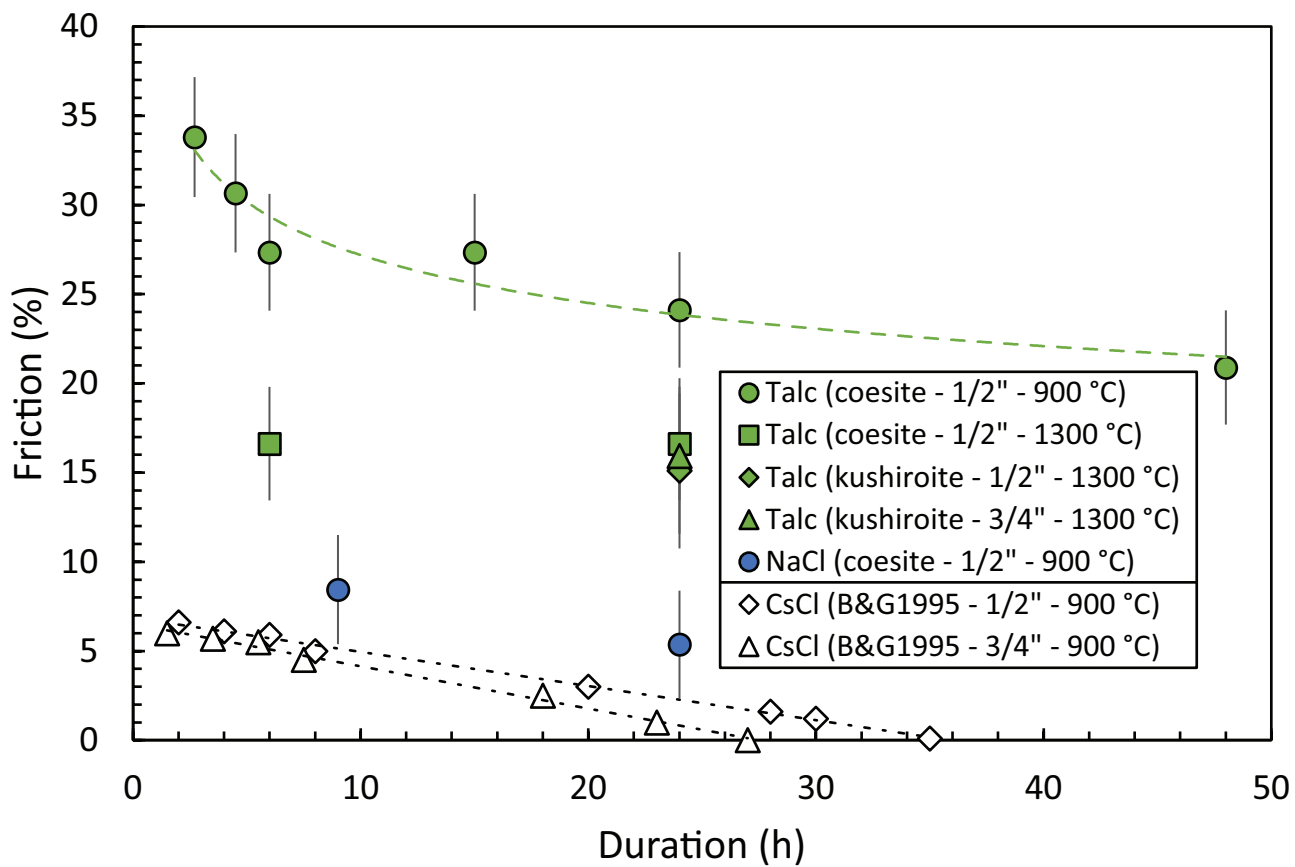


Fig. 4

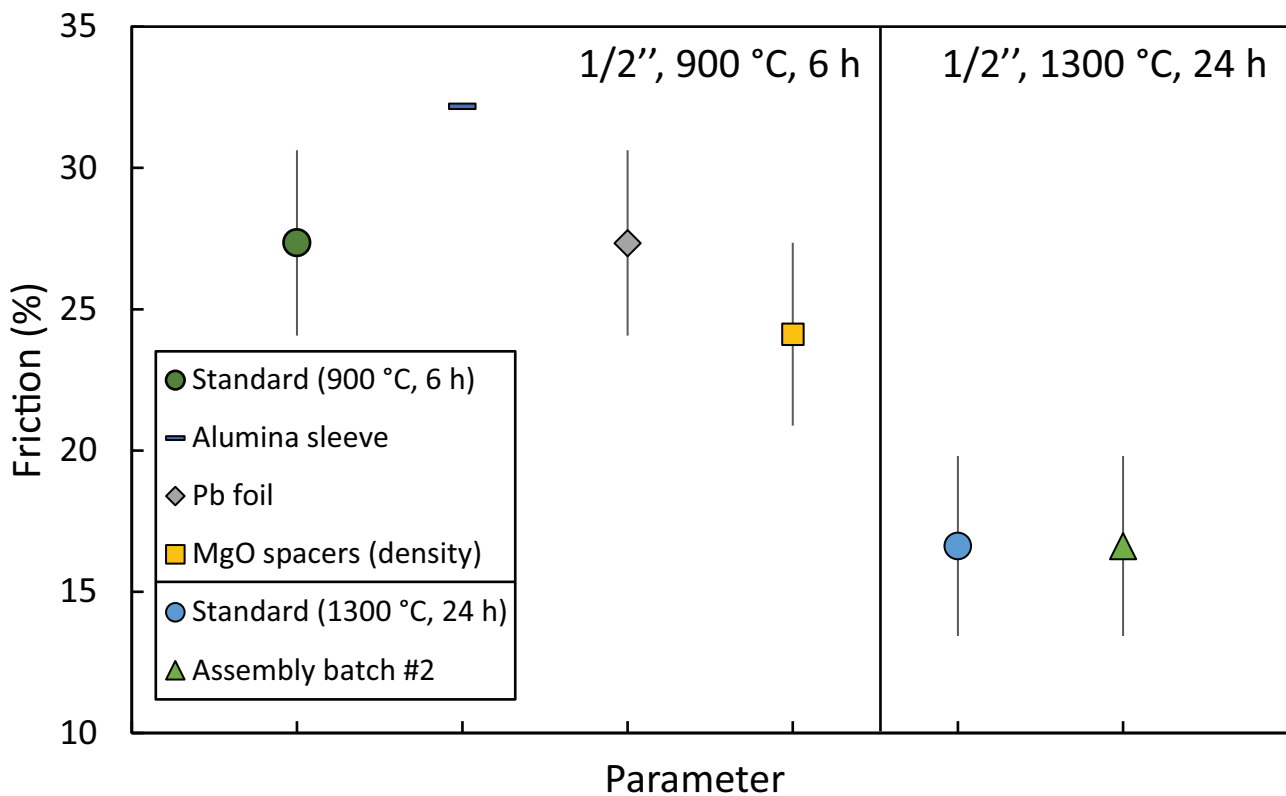


Fig. 5

